
MetaGMT: Improving Actionable Interpretability of Graph Multilinear Networks via Meta-Learning Filtration

Rishabh Bhattacharya¹ Hari Shankar¹ Vaishnavi Shivkumar¹ Ponnurangam Kumaraguru¹

Abstract

The growing adoption of Graph Neural Networks (GNNs) in high-stakes domains like healthcare and finance demands reliable explanations of their decision-making processes. While inherently interpretable GNN architectures like Graph Multilinear Networks (GMT) have emerged, they remain vulnerable to generating explanations based on spurious correlations, potentially undermining trust in critical applications. We present MetaGMT, a meta-learning framework that enhances explanation fidelity through a novel bi-level optimization approach. We demonstrate that MetaGMT significantly improves both explanation quality (AUC-ROC, Precision@K) and robustness to spurious patterns, across BA-2Motifs, MUTAG, and SP-Motif benchmarks. Our approach maintains competitive classification accuracy while producing more faithful explanations (with an increase up to 8% of Explanation ROC on SP-Motif 0.5) compared to baseline methods. These advancements in interpretability could enable safer deployment of GNNs in sensitive domains by (1) facilitating model debugging through more reliable explanations, (2) supporting targeted retraining when biases are identified, and (3) enabling meaningful human oversight. By addressing the critical challenge of explanation reliability, our work contributes to building more trustworthy and actionable GNN systems for real-world applications.

1. Introduction

Graph Neural Networks (GNNs) have achieved remarkable success in various domains, including bioinformatics (Gaudelet et al., 2021), finance (Yang et al., 2022), and social network analysis (Fan et al., 2019). However, their

complex, non-linear nature often renders them to be black boxes, hindering trust and adoption, particularly in critical applications where understanding the rationale behind a prediction is paramount (Dwivedi et al., 2023). This has led to significant research into GNN interpretability, aiming to provide insights into their decision-making processes.

We seek to obtain GNN ‘explanations’, which may refer to subgraphs, node features or relational patterns that are critical to the input graph in order to obtain a given prediction. Existing approaches broadly fall into two categories: post-hoc methods that explain pre-trained models (Ying et al., 2019; Luo et al., 2020), and inherently interpretable models that generate explanations concurrently with predictions (Miao et al., 2022; Chen et al., 2024). The latter category often employs attention mechanisms or learns explicit subgraph masks to highlight the most influential parts of the input graph.

Recently, Chen et al. (2024) proposed the Graph Multilinear neT (GMT) framework, offering a principled approach to interpretable subgraph learning based on the Subgraph Multilinear Extension (SubMT). GMT, along with its variants GMT-LIN (linear approximation) and GMT-SAM (sampling-based approximation), represents the state-of-the-art in generating subgraph-based explanations. However, as with many explanation methods, GMT can sometimes highlight subgraphs that are strongly correlated with the prediction outcome but may not align with the underlying decision-making process of the GNN. These correlation-based explanations can affect the interpretability fidelity, potentially leading to misinformed debugging or misguided interventions.

In order to reduce the generation of spurious explanations and consequently enhance the reliability of GNN explanations, we introduce **MetaGMT: Meta-Filtered Graph Multilinear Networks**. Our core idea is to augment the GMT training process with a meta-learning objective inspired by MATE (Spinelli et al., 2021).

Meta-learning, or learning-to-learn (Thrun & Pratt, 1998), trains models on a distribution of tasks to enable rapid adaptation to new tasks. With respect to graph explainability, the meta-objective acts as a filter, steering the optimizer and

¹IIT-Hyderabad, Hyderabad, India. Correspondence to: Rishabh Bhattacharya <rishabh.bhattacharya@research.iiit.ac.in>.

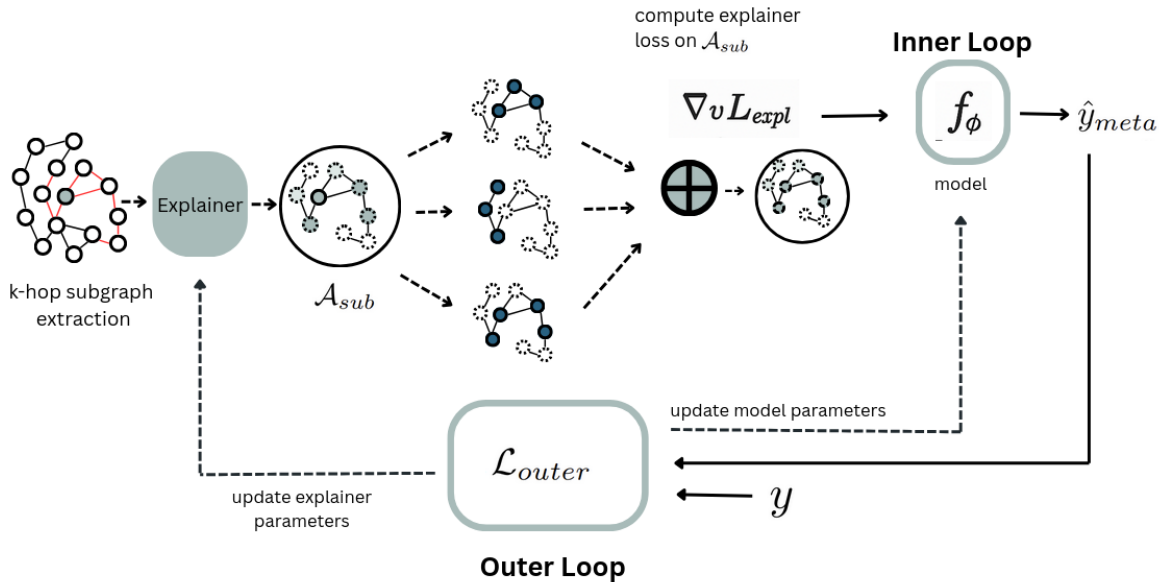


Figure 1. The complete pipeline of MetaGMT. We select a node in the graph and extract its k-hop neighbourhood. Then, we use the explainer to find the attention scores. Using the explanation loss defined in 3 and 4, We iteratively train our model (Inner Loop) to predict the correct class. This prediction is compared to ground truth (Outer Loop), and the loss calculated is used to update our explainer and our model.

implicitly guiding the extractor to learn subgraph explanations that are sparse and predictive. Explanations based on spurious correlations are less likely to facilitate successful adaptation and will thus be penalized by the filter.

We propose and implement MetaGMT, a novel framework enhancing GMT by incorporating a meta-learning filtration step to improve explanation reliability. We demonstrate empirically on different benchmarks (BA-2Motifs, MUTAG, SP-Motif) that MetaGMT improves explanation fidelity (AUC-ROC, Precision@K) while reducing variance across random seeds, resulting in more reliable, actionable graph explanations. Figure 1 summarizes our method.

2. Related Work

2.1. GNN Interpretability

GNN explanation methods aim to identify the crucial input components (nodes, edges, features) driving a model’s prediction. We examine the two broad types of methods detailed in current literature:

Post-hoc methods seek to provide explanations for trained GNNs. GNNExplainer (Ying et al., 2019) optimizes for a subgraph mask maximizing mutual information with the prediction. PGExplainer (Luo et al., 2020) learns a generative model for edge masks, enabling faster explanations. Other approaches include gradient-based methods (Pope et al., 2019), perturbation-based methods (Yuan et al., 2021), and

surrogate models (Vu & Thai, 2020). However, while post-hoc methods are flexible, they may not perfectly reflect the original model’s internal reasoning (Agarwal et al., 2022).

Inherently interpretable methods integrate explanation generation into the model architecture. Attention mechanisms (Veličković et al.; Miao et al., 2022) naturally provide importance scores, often regularized for sparsity. GSAT (Miao et al., 2022) uses stochastic gates and information bottleneck principles. SUNNY-GNN (Deng & Shen, 2023) aims for sufficient and necessary explanations via contrastive learning. Recently, Chen et al. (2024) introduced the Subgraph Multilinear Extension (SubMT) as a theoretical foundation and proposed GMT (GMT-LIN and GMT-SAM), which directly approximates SubMT to learn subgraph distributions, achieving state-of-the-art explanation fidelity. Our work directly builds upon and aims to enhance the GMT framework.

2.2. Meta-Learning for Explainability and Graphs

In the context of graph explainability, Spinelli et al. (2021) proposed MATE (Meta-learning Approach for Training Explainable GNNs), which employs a bi-level optimization framework. The inner loop adapts a GNN using explanations from a post-hoc method (such as GNNExplainer) for sampled nodes, while the outer loop updates the GNN to learn representations that are easier to explain. Although MATE enhances a standard GNN’s explainability, it does so externally to the model’s predictive process.

In contrast, our MetaGMT adopts a similar bi-level structure, but applies it to filter explanations produced by an inherently interpretable model (GMT), thereby directly improving the relevance and fidelity of the learned explanations.

Notably, MATE’s reliance on post-hoc explainers presents limitations. Since these methods operate independently of the model’s core reasoning, their explanations are not inherently faithful and may vary significantly across random seeds or input perturbations. In comparison, MetaGMT directly refines the model’s internal explanation mechanism through meta-learning, encouraging alignment with the decision logic. By penalizing correlations that do not contribute meaningfully to the prediction, MetaGMT produces explanations that are more robust, faithful, and tightly coupled with the model’s reasoning.

3. Preliminaries: Graph Multilinear Networks

Graph Multilinear neT (GMT) (Chen et al., 2024) aims to learn an interpretable subgraph distribution for a given input graph $G = (V, E)$ with node features X and potentially edge features E_{attr} .

3.1. Subgraph Multilinear Extension (SubMT)

GMT is motivated by the Subgraph Multilinear Extension (SubMT). Let $S \subseteq E$ be a subgraph defined by a subset of edges. Let $f(S)$ be a score associated with subgraph S (e.g., the GNN’s prediction probability given only edges in S). The multilinear extension $F : [0, 1]^{|E|} \rightarrow \mathbb{R}$ of f is defined for a vector $p \in [0, 1]^{|E|}$ (where p_e is the probability of including edge e) as:

$$F(p) = \sum_{S \subseteq E} f(S) \prod_{e \in S} p_e \prod_{e' \in E \setminus S} (1 - p_{e'}) \quad (1)$$

This represents the expected score over subgraphs sampled according to the edge probabilities p . GMT aims to learn edge probabilities p (represented by attention scores) such that the resulting SubMT value $F(p)$ is optimized for the downstream task, while also encouraging sparsity in p for interpretability.

3.2. GMT Framework

GMT employs two main components:

1. **Classifier GNN (\mathcal{M}_{clf}):** A standard GNN such as a GIN or GCN (Xu et al., 2019; Kipf & Welling, 2016) mapping $(G, X) \rightarrow Y$, optionally with edge attention weights.
2. **Extractor (\mathcal{M}_{ext}):** An MLP producing edge logits $\mathcal{A}_{log} \in \mathbb{R}^{|E|}$ from node embeddings, with $\mathcal{A} = \sigma(\mathcal{A}_{log})$.

The training objective combines a prediction loss and an information loss (promoting sparsity):

$$\mathcal{L}_{GMT} = \mathcal{L}_{pred}(\mathcal{M}_{clf}(G, \mathcal{A}), y) + \lambda \mathcal{L}_{info}(\mathcal{A}) \quad (2)$$

where y is the ground truth label, \mathcal{L}_{pred} is typically cross-entropy, λ is a balancing coefficient, and \mathcal{L}_{info} is an information-theoretic regularizer (e.g., KL divergence between the attention distribution \mathcal{A} and a target sparsity prior r):

$$\mathcal{L}_{info}(\mathcal{A}) = \mathbb{E}_{e \sim \mathcal{A}} \left[\log \frac{a_e}{r} + \log \frac{1 - a_e}{1 - r} \right] \quad (3)$$

The target sparsity r can be annealed during training.

3.3. GMT Variants

Chen et al. (2024) propose two variants for integrating attention \mathcal{A} into the classifier:

- **GMT-LIN:** Directly applies continuous attention scores \mathcal{A} within GNN layers, linearly approximating SubMT with a single forward pass.
- **GMT-SAM:** Draws multiple binary masks $\hat{\mathbb{I}}^{(i)} \sim \text{Bernoulli}(\mathcal{A})$ and averages predictions: $\hat{y} = \frac{1}{K} \sum_{i=1}^K \mathcal{M}_{clf}(G, \hat{\mathbb{I}}^{(i)})$. This yields a better SubMT approximation but incurs higher computational cost.

4. MetaGMT: Meta-Filtered GMT

While GMT provides a strong baseline for interpretable subgraph learning, the learned attention masks \mathcal{A} can still highlight edges that are spuriously correlated with the label rather than being truly explanatory. This limits the faithfulness and reliability of the resulting explanations.

To address this, we propose MetaGMT, which enhances GMT with a meta-learning-based filtration strategy. The key idea is to encourage explanations that are not just predictive within a local subgraph but also generalizable to the full graph. Rather than relying solely on static loss functions, MetaGMT evaluates the utility of explanations dynamically—penalizing those that fail to support consistent model behavior across contexts. The following subsections formalize this idea. We summarize our pipeline in Figure 1.

4.1. Rationale: Filtration via Meta-Adaptation

Let $G = (V, E)$ be an input graph, and $G_{sub} \subset G$ be a k -hop subgraph centered at node $v \in V$. Given attention scores \mathcal{A}_{sub} produced by the extractor \mathcal{M}_{ext} , a local explanation is defined by a sparse mask over E_{sub} . Intuitively, if this explanation captures the true decision-relevant structure, then adapting the classifier \mathcal{M}_{clf} using \mathcal{A}_{sub} should improve performance on the original graph G .

Algorithm 1 MetaGMT Training Step

-
- 1: **Input:**
 - Graph $G = (X, V, E)$, label y
 - Classifier $\mathcal{M}_{clf}(\theta_{clf})$, extractor $\mathcal{M}_{ext}(\theta_{ext})$
 - Inner learning rate α , outer optimizer Opt_{outer}
 - Inner steps N_{inner} , hops k
 - 2: Sample node $v \in V$.
 - 3: Extract k -hop subgraph G_{sub} around v .
 - 4: Compute subgraph attention \mathcal{A}_{sub} using $\mathcal{M}_{ext}(\theta_{ext})$.
 - 5: Initialize functional classifier parameters $\phi_{clf}^{(0)} \leftarrow \theta_{clf}$.
 - 6: Initialize inner optimizer Opt_{inner} (e.g., SGD) for ϕ_{clf} .
 - 7: **Inner Loop:**
 - 8: **for** $n = 0$ **to** $N_{inner} - 1$ **do**
 - 9: Compute $\mathcal{L}_{expl}(\mathcal{A}_{sub})$ (Eq. 4).
 - 10: Update $\phi_{clf}^{(n+1)} \leftarrow Opt_{inner}(\phi_{clf}^{(n)}, \nabla_{\phi_{clf}^{(n)}} \mathcal{L}_{expl})$.
 - 11: **end for**
 - 12: Let $\phi_{clf}^* = \phi_{clf}^{(N_{inner})}$.
 - 13: **Outer Loop:**
 - 14: Compute meta-prediction $\hat{y}_{meta} = \mathcal{M}_{clf}(\phi_{clf}^*)(G)$.
 - 15: Compute outer loss $\mathcal{L}_{outer} = \mathcal{L}_{pred}(\hat{y}_{meta}, y)$.
 - 16: Compute meta-gradients:
 - 17: $g_{clf} = \nabla_{\theta_{clf}} \mathcal{L}_{outer}$
 - 18: $g_{ext} = \nabla_{\theta_{ext}} \mathcal{L}_{outer}$.
 - 19: Update $\theta_{clf} \leftarrow Opt_{outer}(\theta_{clf}, g_{clf})$.
 - 20: Update $\theta_{ext} \leftarrow Opt_{outer}(\theta_{ext}, g_{ext})$.
-

Conversely, explanations relying on spurious correlations will degrade full-graph performance when used for adaptation. MetaGMT exploits this principle by filtering explanations through a bi-level optimization loop, described in the next section, where the outer loss on G provides feedback on the quality of explanations used in the inner loop.

4.2. Bi-Level Optimization

We train the model architectures from scratch. Let θ_{clf} be the parameters of the classifier \mathcal{M}_{clf} and θ_{ext} be the parameters of the extractor \mathcal{M}_{ext} . The standard GMT training updates both θ_{clf} and θ_{ext} based on \mathcal{L}_{GMT} (Eq. 2). MetaGMT modifies this update as follows for each training batch (or graph) G :

1. Inner Loop: Classifier Adaptation on Subgraph

The process begins by sampling a node $v \in V$ uniformly at random. From this node, the k -hop computational subgraph $G_{sub} = (V_{sub}, E_{sub})$ centered around v is extracted, where X_{sub} and $E_{attr,sub}$ denote the corresponding node and edge features, respectively (in our implementation, $k = 1$). The original extractor $\mathcal{M}_{ext}(\theta_{ext})$ then processes

the initial node embeddings of the subgraph to compute attention logits $\mathcal{A}_{log,sub}$ and normalized attention scores $\mathcal{A}_{sub} = \sigma(\mathcal{A}_{log,sub})$ for the edges E_{sub} , based on the initial node representations $\langle \cdot \rangle_{sub}^{(0)}$.

An explanation loss \mathcal{L}_{expl} is defined on the subgraph, specifically using the information loss (Eq. 3) applied to the subgraph attention scores:

$$\mathcal{L}_{expl}(\mathcal{A}_{sub}) = \mathcal{L}_{info}(\mathcal{A}_{sub}) \quad (4)$$

This loss encourages the extractor to produce sparse and focused attention patterns, even within the local subgraph context.

Next, a functional copy of the classifier \mathcal{M}_{clf} is created with parameters ϕ_{clf} , initialized to the original classifier parameters θ_{clf} . The inner loop adaptation consists of N_{inner} steps, where ϕ_{clf} is updated using an inner optimizer (e.g., SGD with learning rate α) to minimize \mathcal{L}_{expl} :

$$\phi_{clf}^{(n+1)} = \phi_{clf}^{(n)} - \alpha \nabla_{\phi_{clf}^{(n)}} \mathcal{L}_{expl}(\mathcal{A}_{sub}) \quad (5)$$

The final adapted parameters after N_{inner} steps are denoted by $\phi_{clf}^* = \phi_{clf}^{(N_{inner})}$. The inner-loop optimization updates ϕ_{clf} , while the extractor parameters θ_{ext} remain fixed throughout the adaptation process.

2. Outer Loop: Meta-Update on Full Graph

We apply the adapted classifier $\mathcal{M}_{clf}(\phi_{clf}^*)$ to the original full graph G , yielding the prediction $\hat{y}_{meta} = \mathcal{M}_{clf}(\phi_{clf}^*)(G)$. The adapted classifier retains the original extractor $\mathcal{M}_{ext}(\theta_{ext})$ to generate attention weights \mathcal{A} for the full graph during its forward pass, consistent with the standard GMT forward pass.

Next, we compute the standard classification loss on the full graph using the adapted classifier’s prediction:

$$\mathcal{L}_{outer} = \mathcal{L}_{pred}(\hat{y}_{meta}, y) \quad (6)$$

The gradients of \mathcal{L}_{outer} with respect to the original parameters θ_{clf} and θ_{ext} are then calculated. The ‘higher’ library facilitates this by automatically backpropagating through the inner loop adaptation steps, producing:

$$g_{clf} = \nabla_{\theta_{clf}} \mathcal{L}_{outer} \quad ; \quad g_{ext} = \nabla_{\theta_{ext}} \mathcal{L}_{outer} \quad (7)$$

Finally, the original parameters are updated using the main optimizer, such as Adam with learning rate β :

$$\theta_{clf} \leftarrow \text{OptimizerUpdate}(\theta_{clf}, g_{clf}) \quad (8)$$

$$\theta_{ext} \leftarrow \text{OptimizerUpdate}(\theta_{ext}, g_{ext}) \quad (9)$$

The overall process is summarized in Algorithm 1.

5. Experiments

5.1. Experimental Setup

Dataset: We use the BA-2Motifs (Ying et al., 2019), MUTAG (Zhang et al., 2019) and Sp-Motif (Wang et al.) benchmarks to evaluate our methodology. BA-2Motifs is a synthetic benchmark commonly used for evaluating GNN explanation methods. It consists of Barabási-Albert (BA) graphs where specific “house” or “cycle” motifs are attached. The task is graph classification based on the presence of the motif. Ground truth edge explanations correspond to the edges forming the attached motif.

MUTAG is a real-world benchmark dataset for graph classification, consisting of 188 molecular graphs representing nitroaromatic compounds. Each graph corresponds to a chemical compound where nodes represent atoms and edges represent chemical bonds. The primary classification task is to predict the mutagenicity of these compounds, i.e., their potential to cause mutations in the DNA of Salmonella typhimurium. Ground truth explanations often correspond to specific chemical substructures such as carbon rings containing NH_2 or NO_2 groups that are known to be mutagenic.

SP-Motif is a synthetic benchmark designed to evaluate graph learning methods under distribution shifts and spurious correlations. Each graph in SP-Motif consists of two parts: a variant base subgraph and an invariant motif subgraph. The graph label depends solely on the motif subgraph, which represents the true causal structure, while the base subgraph is spuriously correlated with the label during training. SP-Motif additionally provides a parameter b that controls the degree of spurious correlation between the non-causal base subgraph and the graph label during training. The parameter b determines the probability that a training sample’s base structure (e.g., a tree, wheel, or ladder) aligns with the label, even though the label is causally determined only by the motif.

We present our results for GMT-LIN on SP-Motif with three different configurations: $b = 0.5$, $b = 0.7$ and $b = 0.9$. For GMT-SAM we present our results for $b = 0.5$, and include runs for $b = 0.7$ and $b = 0.9$ in the GitHub repository¹.

Baselines: We compare our meta-filtered variants, MetaGMT-LIN and MetaGMT-SAM, against their respective vanilla methods, GMT-LIN and GMT-SAM (Chen et al., 2024), trained using the standard objective (Eq. 2).

Implementation: We adapt the official GMT implementa-

¹Code available at <https://anonymous.4open.science/r/goddammit-sparky-F9DB/>

tion based on PyTorch Geometric (Fey & Lenssen, 2019). The backbone GNN classifier uses a GIN architecture. The extractor is an MLP. Key meta-parameters were set as follows: inner steps $N_{inner} = 3$, inner learning rate $\alpha = 0.01$, subgraph hops $k = 1$. Other hyperparameters (outer learning rate, loss coefficients, sparsity schedule, etc.) were kept consistent between the baseline GMT and MetaGMT variants, following the optimal settings reported for GMT on datasets where applicable, or tuned slightly on a validation set. We report results averaged over 10 different seeds, from 0 to 9.

Evaluation Metrics: We evaluate both explanation quality and classification performance:

- **Explanation AUC (X-ROC):** Area Under the ROC Curve comparing the learned edge attention scores against the ground truth motif edge labels. Measures explanation fidelity.
- **Explanation Precision@K (X-Prec@K):** Precision of the top-K predicted edges based on attention scores, compared to ground truth motif edges. We use $K=5$, matching the typical motif size. Measures explanation accuracy for the most salient edges.
- **Classification Accuracy (Clf-Acc):** Standard graph classification accuracy on the test set.

We report the metrics achieved at the epoch yielding the best validation classification accuracy.

5.2. Results

Tables 1 and 2 present comprehensive performance comparisons between GMT-LIN and our proposed MetaGMT-LIN variants across BA-2Motifs, MUTAG, and Spurious-Motif benchmarks.

Our results demonstrate consistent improvements in both interpretation quality and model robustness. On BA-2Motifs, MetaGMT-LIN achieves superior interpretation performance with 98.37% X-ROC (compared to 97.97% for GMT-LIN) and 91.96% X-Prec@5 (vs 88.58%).

The stability of explanations shows notable enhancement across all benchmarks. For BA-2Motifs, the standard deviation of X-Prec@5 decreases from ± 10.60 for GMT-LIN to just ± 3.79 for MetaGMT-LIN, indicating significantly more consistent explanation quality. This pattern holds for the Spurious-Motif benchmark, where MetaGMT-LIN achieves both higher mean scores and lower variance compared to baseline methods.

The performance improvements are particularly pronounced in challenging scenarios with higher bias levels in the Spurious-Motif benchmark. At bias level 0.7, MetaGMT-LIN achieves 80.16% X-ROC (± 8.28) compared to 72.14%

Table 1. Interpretation Performance (ROC) across BA-2Motifs, MUTAG and Spurious-Motif benchmarks. Methods having better performance are highlighted in bold. Results highlight the robustness of MetaGMT-LIN compared to baseline GMT-LIN, particularly in high-bias settings (SP-Motif, $b = 0.9$), where leveraging meta-learning improves invariance to spurious features. Performance on BA-2Motifs and MUTAG (alternative benchmarks) is included for reference, showing consistent competitiveness. Standard deviations reflect stability across different seeds (0-9 inclusive).

	BA-2MOTIFS	MUTAG	SPURIOUS-MOTIF		
			B = 0.5	B = 0.7	B = 0.9
GMT-LIN	97.97 ± 1.46	93.13 ± 2.06	72.62 ± 7.99	72.14 ± 14.89	66.84 ± 12.36
METAGMT-LIN	98.37 ± 1.08	92.60 ± 2.05	80.04 ± 2.76	80.16 ± 8.28	69.59 ± 4.18

Table 2. Explanation Precision @ 5 (X-Prec@5) across BA-2Motifs, MUTAG and Spurious-Motif benchmarks. Methods having better performance are highlighted in bold. MetaGMT-LIN demonstrates superior robustness at $b = 0.9$, outperforming baselines by 9% (50.79 vs. 41.85), suggesting better avoidance of spurious explanations. On BA-2Motifs, MetaGMT-LIN achieves high precision (> 88%), while MUTAG (real-world) results reflect inherent task difficulty. Standard deviations highlight variance across seeds.

	BA-2MOTIFS	MUTAG	SPURIOUS-MOTIF		
			B = 0.5	B = 0.7	B = 0.9
GMT-LIN	88.58 ± 10.60	28.66 ± 1.38	46.34 ± 6.43	48.66 ± 13.13	41.85 ± 9.29
METAGMT-LIN	91.96 ± 3.79	28.55 ± 1.92	48.48 ± 2.96	57.82 ± 9.71	50.79 ± 6.12

(±14.89) for GMT-LIN, demonstrating both higher performance and greater stability in the presence of confounding factors. All metrics have been reported in Tables 1 and 2.

Tables 3 and 4 present performance comparisons between GMT-SAM and the proposed MetaGMT-SAM. Overall, MetaGMT-SAM shows slight improvements over GMT-SAM in ROC scores on BA-2Motifs (97.83 vs. 97.13) and Spurious-Motif (79.25 vs. 73.78), indicating enhanced interpretability. However, it performs marginally worse on MUTAG (93.58 vs. 94.79). In terms of X-Prec@5, GMT-SAM slightly outperforms MetaGMT-SAM on BA-2Motifs and Spurious-Motif ($b = 0.5$), while both models yield nearly identical results on MUTAG. These results suggest that Meta-learning benefits ROC-based interpretation performance more consistently than precision-based explanation accuracy.

Table 3. ROC-AUC scores comparing GMT-SAM and MetaGMT-SAM across benchmarks. Methods having better performance are highlighted in bold. MetaGMT-SAM shows consistent improvements on synthetic datasets, achieving +0.7% on BA-2Motifs (97.83 vs 97.13) and a more substantial +5.47% gain on SP-Motif with $b=0.5$ (79.25 vs 73.78), demonstrating better robustness to spurious correlations.

	BA-2MOTIFS	MUTAG	SP-MOTIF (B = 0.5)
GMT-SAM	97.13 ± 1.28	94.79 ± 2.07	73.78 ± 8.82
METAGMT-SAM	97.83 ± 1.65	93.58 ± 3.10	79.25 ± 3.07

These results collectively demonstrate that our proposed methodology not only enhances explanation fidelity and classification accuracy but also significantly reduces performance variability across different seeds and data splits. Consistent improvements across multiple benchmarks and

Table 4. Explanation Precision@5 comparison for GMT-SAM and MetaGMT-SAM. Methods having better performance are highlighted in bold. MetaGMT-SAM achieves higher precision on BA-2Motifs (91.72 vs 90.36) with lower variance (±2.70 vs ±3.77), suggesting more reliable explanations for synthetic graphs. On SP-Motif ($b=0.5$), GMT-SAM shows marginally better performance (50.14 vs 48.72) but with nearly double the standard deviation (7.83 vs 3.63), making MetaGMT-SAM’s explanations more consistent.

	BA-2MOTIFS	MUTAG	SP-MOTIF (B = 0.5)
GMT-SAM	90.36 ± 3.77	28.65 ± 1.43	50.14 ± 7.83
METAGMT-SAM	91.72 ± 2.70	28.48 ± 1.92	48.72 ± 3.63

metrics suggest that the meta-learning filtration step provides superior generalization capabilities on unseen data.

6. Discussion

Consistent improvements in explanation fidelity metrics (X-ROC, X-Prec@5) suggest that the meta-learning filtration mechanism successfully guides the extractor to focus on edges that are more aligned with the ground truth motifs. By rewarding explanations that facilitate robust classifier adaptation from local subgraphs to the global graph, MetaGMT effectively filters out potentially spurious edges that might be captured by the standard GMT objective alone.

This enhanced reliability is crucial for actionable interpretability. We list some of the potential use cases below:

- **Model Debugging:** If the model makes an error, a high-fidelity explanation is more likely to pinpoint the correct cause (e.g., a missing or distorted motif), en-

abling targeted corrections. In contrast, a misleading explanation might send developers in the wrong direction.

- **Scientific Discovery:** In domains like drug discovery or materials science, identifying the true structural drivers of a property is critical. More faithful and robust explanations improve the likelihood of discovering meaningful structure-property relationships.
- **Trust and Verification:** Users are more likely to trust and rely on explanations that consistently highlight relevant features across varying contexts.
- **Model Retraining and Deployment:** Reliable explanations can guide selective model editing and retraining, allowing developers to iteratively improve generalization or correct failure modes without exhaustive manual inspection.

Our experiments further show that improvements in interpretability come with either preserved or slightly improved predictive performance, indicating that the meta-learning objective helps regularize the model in a way that benefits both explanation quality and robustness. This robustness is particularly important in real-world deployments, where consistent performance across retraining runs or environments is crucial.

The meta-objective provides a self-supervised signal for explanation quality, rooted in internal consistency and adaptability. It encourages the model to favor explanations that are not only faithful but also useful, thus aligning with the goals of actionable interpretability and practical impact.

7. Limitations and Future Work

Incorporating a meta-learning filtration step in the standard GMT training step comes with a notable increase in computational cost, due to the bi-level optimization taking place at each epoch. Consequently, the computational cost scales with the number of inner loop adaptation steps. Our experimental setup used a fixed number of inner steps $N_{inner} = 3$ for all datasets.

In practice, incorporating a bi-level optimization method, by means of meta-learning, we introduce a trade-off between the benefits of meta-learning for improved interpretability and the computational overhead required during training, necessitating careful consideration of resource constraints when implementing MetaGMT.

By producing more robust, reliable explanations, MetaGMT contributes to the goal of actionable interpretability for GNNs. Future work includes evaluating MetaGMT on more complex real-world datasets, exploring different formulations of the inner-loop explanation loss, and investigating

the computational trade-offs of the meta-learning approach. We believe that integrating principles of adaptation and generalization, as done in MetaGMT, is a promising direction for developing GNN explanation methods that are not just interpretable, but truly trustworthy and actionable. Trustworthy explanations may be beneficial for the adaptation of such models for tasks in various domains such as e-commerce, social networks, recommendation systems, etc.

Impact Statement

This paper presents work whose goal is to advance the field of Machine Learning, specifically in the area of Graph Neural Network interpretability. By improving the reliability and actionability of GNN explanations, our work aims to foster greater trust and enable more responsible deployment of GNNs in critical applications such as healthcare, finance, and scientific discovery. While improved interpretability can lead to positive societal outcomes through better model understanding and debugging, potential negative consequences could arise if misinterpreted or over-relied upon explanations lead to flawed decisions. We believe the primary impact is positive, contributing to more transparent and trustworthy AI systems. There are many potential societal consequences of our work, none which we feel must be specifically highlighted here beyond the general implications of advancing interpretable machine learning.

References

- Agarwal, C., Lakkaraju, H., and Zitnik, M. Evaluating explainability for graph neural networks. In *Advances in Neural Information Processing Systems (NeurIPS)*, volume 35, pp. 35528–35541, 2022.
- Chen, Y., Bian, Y., Han, B., and Cheng, J. How interpretable are interpretable graph neural networks? In *International Conference on Machine Learning (ICML)*, 2024. URL <https://arxiv.org/abs/2406.07955>.
- Deng, Z. and Shen, Y. Self-interpretable graph learning with sufficient and necessary explanations. In *Proceedings of the AAAI Conference on Artificial Intelligence*, volume 37, pp. 16721–16729, 2023.
- Dwivedi, R., Yuan, H., Yu, S., Tan, C., and Luo, J. Explainable graph neural networks: A survey. *ACM Transactions on Knowledge Discovery from Data*, 17(8):1–50, 2023.
- Fan, W., Ma, Y., Li, Q., He, Y., Zhao, E., Tang, J., and Yin, D. Graph neural networks for social recommendation. In *The World Wide Web Conference*, pp. 417–426, 2019.
- Fey, M. and Lenssen, J. E. Fast graph representation learning

- with pytorch geometric. In *ICLR Workshop on Representation Learning on Graphs and Manifolds*, 2019.
- Gaudelet, T., Mallet, V., Mineva, T., et al. Utilising graph machine learning within drug discovery and development. *Briefings in Bioinformatics*, 22(6):bbab159, 2021.
- Kipf, T. N. and Welling, M. Semi-supervised classification with graph convolutional networks. *arXiv preprint arXiv:1609.02907*, 2016.
- Luo, D., Cheng, W., Xu, D., Yu, W., Zong, B., Chen, H., and Zhang, X. Parameterized explainer for graph neural network. In *Advances in Neural Information Processing Systems (NeurIPS)*, volume 33, pp. 19708–19719, 2020.
- Miao, S., Pan, S., Zhao, X., Zheng, Y., Wang, X., and Yu, P. S. Interpretable and generalizable graph learning via stochastic attention mechanism. In *International Conference on Machine Learning (ICML)*, pp. 15678–15691. PMLR, 2022.
- Pope, P. E., Kolouri, S., Rostami, M., Martin, C. E., and Hoffmann, H. Explainability methods for graph convolutional neural networks. In *Proceedings of the IEEE/CVF conference on computer vision and pattern recognition*, pp. 10772–10781, 2019.
- Spinelli, I., Scardapane, S., and Uncini, A. A meta-learning approach for training explainable graph neural networks. *IEEE Transactions on Neural Networks and Learning Systems*, 2021. URL <https://arxiv.org/abs/2109.09426>.
- Thrun, S. and Pratt, L. Learning to learn. *Kluwer Academic Publishers*, 1998.
- Veličković, P., Cucurull, G., Casanova, A., Romero, A., Lio, P., and Bengio, Y. Graph attention networks. In *International Conference on Learning Representations (ICLR)*.
- Vu, M. and Thai, M. T. Pgm-explainer: Probabilistic graphical model explanations for graph neural networks. In *Advances in Neural Information Processing Systems (NeurIPS)*, volume 33, pp. 12039–12050, 2020.
- Wang, Y., Chen, Y., Huang, J., Liu, Z., Zhang, J., Cheng, X., Li, Y., and Zhong, Z. Learning invariant graph representations via virtual environment inference.
- Xu, K., Hu, W., Leskovec, J., and Jegelka, S. How powerful are graph neural networks? In *International Conference on Learning Representations (ICLR)*, 2019.
- Yang, J., Liu, Z., Zhao, W., Zhang, Z., and Cui, B. Graph neural network for fraud detection: A review and prospect. In *Proceedings of the 31st ACM International Conference on Information & Knowledge Management*, pp. 4978–4982, 2022.
- Ying, R., Bourgeois, D., You, J., Zitnik, M., and Leskovec, J. GNNExplainer: Generating explanations for graph neural networks. In *Advances in Neural Information Processing Systems (NeurIPS)*, volume 32, 2019.
- Yuan, H., Yu, H., Gui, S., and Ji, S. On explainability of graph neural networks via subgraph explorations. In *International Conference on Machine Learning (ICML)*, pp. 12241–12252. PMLR, 2021.
- Zhang, Z., Bu, J., Ester, M., Zhang, J., Yao, C., Yu, Z., and Wang, C. Hierarchical graph pooling with structure learning. *arXiv preprint arXiv:1911.05954*, 2019.

A. Appendix

A.1. Classification Accuracy

Table 5. Classification Accuracy (Clf-Acc) across BA-2Motifs, MUTAG and Spurious-Motif benchmarks. GMT-LIN outperforms MetaGMT-LIN in high-bias scenarios ($b = 0.9$), with GMT-LIN achieving 66.90% accuracy compared to MetaGMT-LIN’s 54.53%, suggesting potential trade-offs between classification performance and explanation quality in biased settings.

	BA-2MOTIFS	MUTAG	SPURIOUS-MOTIF		
			B = 0.5	B = 0.7	B = 0.9
GMT-LIN	99.20 \pm 0.98	91.56 \pm 0.85	75.13 \pm 1.22	69.37 \pm 1.67	66.90 \pm 4.48
METAGMT-LIN	99.50 \pm 0.50	91.12 \pm 1.05	71.64 \pm 1.97	65.00 \pm 3.51	54.53 \pm 2.09

MetaGMT-LIN achieves equal or superior accuracy to their baseline counterparts on the BA-2Motifs dataset. Notably, the method shows significantly reduced variance compared to the baselines, particularly for GMT-SAM where the standard deviation decreases from ± 2.40 to just ± 0.66 .

For the MUTAG benchmark, classification accuracies remain stable between baseline and MetaGMT variants, with all methods achieving between 90.07% and 91.56% accuracy. The minor differences ($\leq 1.5\%$) suggest that our meta-learning approach maintains strong discriminative performance while improving explanation quality.

Results on the Spurious-Motif benchmark indicate a potential trade-off pattern. While MetaGMT variants show slightly lower mean accuracy (71.42%-71.64% vs 75.13%-75.49% at $b=0.5$), they maintain more consistent performance as bias increases, as evidenced by smaller accuracy drops across bias levels. This suggests our method may sacrifice marginal classification performance for greater robustness against spurious correlations.

A.2. Hyperparameter Details

Tables 6 and 7 summarize our experimental configurations. Following the GMT framework established by Chen et al. (2024), we maintain consistent hyperparameters where applicable while adapting specific settings (learning rates, attention mechanisms, and sparsity thresholds) to each benchmark’s characteristics.

Table 6. Common hyperparameters across all benchmarks

Parameter	Value
Architecture	
Backbone	GIN (2 layers, 64 dim)
Dropout	0.3
Extractor dropout	0.5
Training	
Precision@K	5
Visualization interval	Every 10 epochs
Training epochs	100
$\lambda_{pred}, \lambda_{info}$	1, 1
Sparsity decay schedule	-0.1 every 10 epochs

Table 7. Dataset-specific configurations

Parameter	BA-2Motifs	MUTAG	SP-Motif
Data			
Split	80/10/10	80/10/10	-
Batch size	128	128	128
Training			
Pretrain lr	1e-3	1e-3	3e-3
Learning rate	1e-3	1e-3	3e-3
Options			
Use Edge Attention	Yes	No	Yes
Sparsity			
Initial r	1.0	1.0	1.0
Final r	0.5	0.5	0.7